PROCEEDINGS, 46th Workshop on Geothermal Reservoir Engineering
Stanford University, Stanford, California, February 16-18, 2021
SGP-TR-217

Impact of Particle Size Distribution on Fracture Sealing Capability; A Simulation for Better Geothermal Drilling

Lu Lee and Arash Dahi Taleghani

Penn State University, University Park, PA 16802

Email: arash.dahi@psu.edu

Keywords: fracture sealing; lost circulation; CFD-DEM; drilling fluid; particle size distribution

ABSTRACT

Lost circulation is one of the major obstacles in drilling wells, especially in geothermal systems with large natural fractures. Without proper treatments, this can result in problems associated with poor well control and an increase in non-productive time (NPT). An economical treatment involves the inclusion of lost-circulation materials (LCMs) into the drilling formula. The idea is to stop fluid loss by bridging and sealing the permeable paths. Yet, the unpredictive nature and abnormally large fracture sizes in geothermal wells make it difficult in stopping the fluid loss. If successful, preventing a severe lost-circulation event can alleviate large drilling costs. Therefore, understanding the fracture sealing function of the LCMs would be invaluable to any drilling operations. Most commonly seen LCMs can be classified as flaky, granular, and fibrous. Ideally, these conventional granular and fibrous LCMs are inert to the mud system. In this paper, the computational fluid dynamics (CFD) and discrete element method (DEM) are coupled as a numerical simulation tool to predict fracture sealing of granular and fibrous particles. One advantage of using the coupled CFD-DEM algorithm is its capability to calculate every single particle motion in an aqueous system by particle-particle and particle-fluid interactions. A smooth permeable channel is created to represent one of many downhole fractures. The success of fracture sealing is heavily dependent on the particle shapes, sizes, and the mechanical strength. The results show better sealing effect on particles with varying sizes than uniformly sized LCMs. Additionally, a mixture of granular and fibrous LCMs can also improve sealing results by reducing fluid losses.

1. INTRODUCTION

Geothermal energy refers to the heat that exists within the earth. It has been receiving growing attentions recently because it is renewable and is considered relatively clean and safe. Proper drilling and completions are necessary for the extraction of the heat resource. Major challenges of drilling a geothermal well include the large fractures and its under-pressured nature in the reservoir. Geothermal reservoirs typically exhibit temperatures from 160 to above 300 °C, high compressive strength of 240+ MPa, and highly fractured formations (Finger and Blankenship, 2010). Therefore, a lost-circulation event is a common occurrence and should be accounted for during the planning phase. The total or partial loss of drilling fluids into highly permeable zones, cavernous formations, and natural or induced fractures can be considered as a lost-circulation problem. A common practice is to add the LCMs into drilling fluid to seal fractures. The goal of this practice is to prevent or remediate the problem depending on its severity. It could lead to stuck pipe, well instability, and loss of well if a lost-circulation event is not properly treated. Economically speaking, lost circulation and its associated problems represent at least an average of 15% increase in well cost at the most mature US geothermal area (Carson and Lin, 1982). Recent studies estimated $185,000 or more is added to the cost (which averaged over 100 hours of unprogrammed nonproductive time) because of lost circulation events (Cole et al., 2017). In conventional reservoirs, drilling fluids account for 25% to 40% of total drilling costs and an extra 10% to 20% may be added to authorizations for expenditures to cover the anticipated downtime (Lecolier et al., 2005; Redden, 2009).

The LCM additives have to be professionally designed, especially in a high-temperature condition. The effectiveness of fracture sealing is heavily dependent on the mechanical strength and the size distribution of the materials, which can be altered by the heat from the geothermal environment. Due to the unpredictive nature of fracture apertures, most of the LCMs used in drilling have shown little effects in preventing loss of circulation. The most commonly seen conventional LCMs can be classified as flaky, fibrous, and granular. Each of them provides different functions in fracture sealing. Granular materials form a porous bridge and reduce the permeability of the loss zone while flaky and fibrous materials form a mat-like bridge over the pore openings (Baret et al., 1990). A mixture of rigid granular particles generally provides the best fracture sealing results (Messenger, 1981). More recent LCM developments such as smart LCMs are designed to expand in a targeted temperature range (Mansour et al. 2017; Mansour and Dahi Taleghani, 2018). There are still challenges for the currently available LCMs to treat fracture apertures in excess of 5 mm (Lavrov, 2016). Nevertheless, if the fracture sealing mechanisms can be understood, a better LCM design criterion or specification could be adapted in treating fluid loss.

Particle size distribution (PSD) is one important design consideration. During the transport process, a bridge inside the fracture is first initiated by the large LCMs, and the interparticle void space is later sealed by the small LCMs. The LCMs experience fast shearing and rapid collisions when pumped downhole. The physical phenomenon such as particle abrasions can be further promoted by the high-temperature environment. Previous simulation studies show how the sealing effectiveness of uniformly sized LCMs changes at elevated temperatures (Lee and Dahi Taleghani, 2020). In this paper, simulation studies are conducted to investigate the sealing capabilities of the particles with different sizes for both granular and non-granular LCMs.

2. THERMAL DEGRADATION ON PARTICLES

2.1 Particle Properties

The LCM particles are subject to thermal degradation. Experimental results show that walnut shells, ground marble, calcium carbonate, and other common LCMs experience a large reduction in particle size in high-temperature drilling fluids (Loeppke et al., 1990; Scott et al., 2012; Kumar et al., 2013; Grant et al., 2016). In addition to temperature, the fluid viscosity, circulation time, rotation speed, particle density and initial size have to be considered for the reduction in the LCMs (Kang et al., 2019). Mechanical properties of geomaterials are found to be sensitive to thermal gradients. Report of commonly used LCMs show various ranges of softening temperatures in **Table 1**. The softening temperatures are measured by slowly increasing particle temperatures under compression in their elastic region of the stress and strain curve. At the softening temperature, the particle strain increases quickly and continues with further increase in temperature until failure occurs.

Table 1: Material properties and the softening temperatures (Loeppke et al., 1990)

Material	Compressive Strength (MPa)	Young's Modulus (MPa)	Softening Temperature (°C / °F)
Thermoset Rubber	14.00	43.64	110-192 / 43-89
Coal	1.45	12.96	250-330 / 121-166
Expanded Aggregate	5.93	44.20	> 500 / > 260
Gilsonite	2.34	12.00	345-375 / 174-191
Mixed Nut Shells	56.74	196.50	380-480 / 193-249
Black Walnut Shells	68.05	141.34	360-500 / 182-260

2.2 Particle Size Distribution

Many LCM blends follow guidelines based on empirical measurements and field experiences. Abrams (1977) states that the median particle size of the bridging materials should be equal or slightly larger than one-third of the median pore size. Others also indicate a rule for maximum particle diameter to be one-half of the fracture width and 5% fluid volume to be the bridging size (Goodman, 1981). Some researchers tested the sealing effectiveness of LCMs based on the maximum density theory (Furnas, 1931) and noticed that the idea of one-third rule is only applicable to the size requirements for initiating a bridge. The ideal packing theory from Kaeuffer (1973) was later adapted by engineers to achieve minimal fluid loss. Some of the design guidelines found in the literatures are summarized in **Table 2**. However, the transport of the LCMs is a dynamic process from the surface to the downhole environment. Attrition and abrasion of particles are promoted by the increase in temperature. Thermally induced stress and chemical reactions can also further advance particle degradation. Increase in temperature would lead to decrease of viscosity, which indirectly results in more particle collisions. Particles that are broken down into smaller pieces, in a high-temperature condition, can also further promote particle degradation (Arena et al., 1983; Lin and Wey, 2005; Kang et al., 2019).

Table 2: The LCM size design guidelines in existing literatures.

Sources	Suggested LCM Designs				
Abrams (1977)	Median particle size ≥ 1/3 of median pore size				
Smith *et al.* (1996); Dick *et al.* (2000)	Linear relationship of cumulative volume vs $d^{0.5}$				
Chellappah and Aston (2012)	Linear relationship of cumulative volume vs $d^{0.5\text{-}1}$				
Hands *et al.* (1998)	D_{90} = maximum pore size				
Vickers *et al.* (2006)	D_{10} > smallest pore throat	D_{25} = 1/7 of the mean pore throat	D_{50} = +/- 1/3 of the mean pore throat	D_{75} < 2/3 of largest pore throat	D_{90} = largest pore throat
Whifill (2008)	D_{50} = 1/3 pore throat		D_{90} = pore throat		
Alsaba *et al.* (2017)	D_{50} ≥ 3/10 the fracture width		D_{90} ≥ 6/5 the fracture width		
Razavi *et al.* (2016)	Bimodal PSD with appropriate ranges and concentrations of coarse and fine particles				

2.3 Fibrous Particles

Particle geometries provide different functions in preventing and remediating loss of circulation. As mentioned earlier, fibrous LCMs help initiate the bridging process. Development on economical fibrous-granular mixtures to enhance the fracture sealing outcomes and minimize fluid loss rates seem very promising (Amanulla et al., 2019; Yang and Chen, 2020). The addition of fibrous LCMs into granular LCMs could help overcome the inefficiency of fracture plugging by granular LCMs. In order not to plug up downhole equipment, the size of the granular LCMs is limited. If granular solids are too small, severe lost circulation may occur. As shown in **Figure 1**, properly sized particles with fibrous materials could improve the fracture sealing outcome. In the attempt of simulating fibrous materials in the DEM algorithm, spherical particles are bonded together to make a string of fibrous material. The technique of bonding multiple spherical particles allows fibrous materials to be physically flexible. Particle deformation such as bending during particle collisions is also possible. In addition to the fibrous materials, irregular shaped particles can also be created by lumping them together. The bond interactions have been studied and modelled in various disciplines (Potyondy and Cundall, 2004; Guo *et al.*, 2013a; Guo *et al.*, 2013b; Schramm *et al.*, 2019).

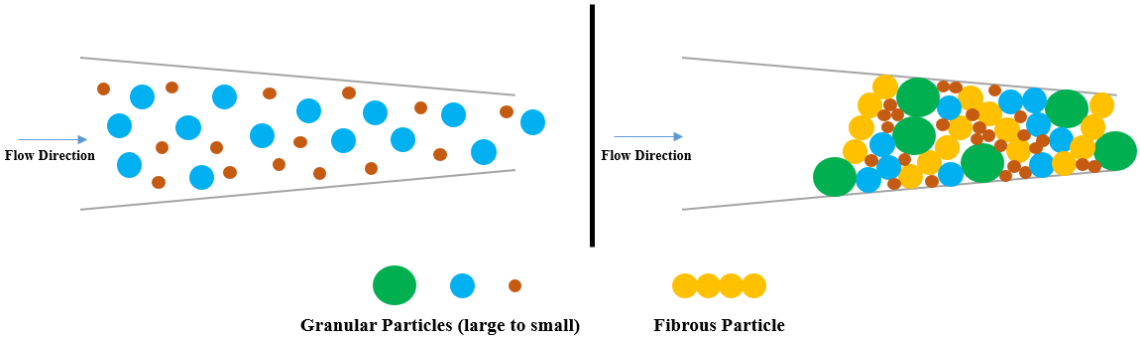

Figure 1: Illustration of inefficient fracture sealing by small particles (left) and successful fracture sealing with proper particle size distribution (right).

3. METHODOLOGY

3.1 Problem Description

The aim of this paper is to study the fracture sealing capability by simulating different particle sizes on both granular and non-granular LCMs. The success of fracture sealing is assessed by the dimensionless fluid loss. The size degradation will be considered due to thermal effect. A fracture with smooth surface is generated for the particulate flow. It is assumed that the fracture walls are rigid and will not deform with any change in pressure. This simplified model can represent a small-scale channel of the fracture network in the reservoir.

3.2 CFD-DEM Coupling

The CFD-DEM coupling can numerically calculate the accurate locations and trajectories of the solid particles inside a fractures. The fluid flow is controlled by the CFD algorithm, and the trajectories of particles are solved by in the DEM algorithm. The two simulation programs are OpenFOAM and LIGGGHTS (Goniva *et al.*, 2012; Kloss *et al.*, 2012). The fundamental theory of CFD-DEM techniques has been comprehensively reviewed in Zhu *et al.* (2007; 2008). Compared to the Eulerian-Eulerian perspective, the Lagrangian way of tracking individual particles in CFD-DEM may help us understand the bridging and sealing process. The Eulerian technique treats the solid particles as a continuous phase, which is efficient in computational power. However, the downside is its sacrifice in the accuracy of particle motions. On the other hand, although the CFD-DEM simulation is a computationally heavy approach, it does provide a great value in generating correct fracture sealing data. For individual particles, Newton's law of motion describes the translational and rotational movements (Cundall and Strack, 1979).

$$m_p \frac{d^2 x_p}{dt^2} = \boldsymbol{F}_{pn} + \boldsymbol{F}_{pt} + \boldsymbol{F}_{pf} + \boldsymbol{F}_{pb} \tag{1}$$

$$I_p \frac{d\boldsymbol{\omega}_p}{dt} = \boldsymbol{r}_{pc} \times \boldsymbol{F}_{pt} + \boldsymbol{T}_{pr} \tag{2}$$

where $\boldsymbol{F}_{pn}$ is the normal contact force, $\boldsymbol{F}_{pt}$ is the tangential contact force, $\boldsymbol{F}_{pf}$ is the force exerted from surrounding fluid to the particles, and $\boldsymbol{F}_{pb}$ is the body force of the particles. For particle rotational motion, I_p is the inertial tensor, $\boldsymbol{r}_{pc}$ is particle radius, and $\boldsymbol{T}_{pr}$ is the additional torque used to model non-sphericity by means of a rolling friction model.

Coupling the DEM with the CFD, the governing equations of unresolved CFD-DEM are described as

$$\frac{\partial \alpha_f}{\partial t} + \nabla \cdot (\alpha_f \boldsymbol{u}_f) = 0 \tag{3}$$

$$\frac{\partial (\alpha_f \rho_f \boldsymbol{u}_f)}{\partial t} + \nabla \cdot (\alpha_f \rho_f \boldsymbol{u}_f \boldsymbol{u}_f) = -\alpha_f \nabla p - K_{pf}(\boldsymbol{u}_f - \boldsymbol{u}_p) + \nabla \cdot (\alpha_f \boldsymbol{\tau}_f) \tag{4}$$

where α_f is the volume fraction of fluid, ρ_f is fluid density, K_{pf} is the implicit momentum exchange term of particle-fluid interactions, $\boldsymbol{u}_f$ is fluid velocity, $\boldsymbol{u}_p$ is the average particle velocity in one specified grid cell, and $\boldsymbol{\tau}_f$ is the stress tensor of fluid.

$$K_{pf} = \frac{\sum_i \boldsymbol{F}_{pf}}{V_{cell}\left|\boldsymbol{u}_f - \boldsymbol{u}_p\right|}, \tag{5}$$

where V_{cell} is the volume of one specified grid cell.

The current model considers the pressure gradient force, the buoyancy force, the viscous force, and the drag force. The Di Felice (1994) drag model is used because of its accuracy for a wide range of Reynolds numbers. The drag force is described as follows.

$$\boldsymbol{F}_{pf} = \frac{1}{8} C_d \rho_f \pi d_p^2 \left(\boldsymbol{u}_f - \boldsymbol{u}_p\right)\left|\boldsymbol{u}_f - \boldsymbol{u}_p\right| \alpha_f^{-\chi} \tag{6}$$

$$C_d = \left(0.63 + \frac{4.8}{\sqrt{Re_p}}\right)^2 \tag{7}$$

$$Re_p = \frac{\alpha_f \rho_f d_p \left|\boldsymbol{u}_f - \bar{\boldsymbol{u}}_p\right|}{\mu} \tag{8}$$

$$\chi = 3.7 - 0.65 e^{-\frac{\left(1.5 - \log_{10} Re_p\right)^2}{2}} \tag{9}$$

where C_d is the drag coefficient, d_p is particle diameter, χ is the empirical constant, Re_p is the particle Reynolds number, and μ is the fluid dynamic viscosity.

In bonded-particle model, the fiber particles are described as follows (Schramm et al., 2019).

$$\Delta \boldsymbol{F}_{n,i}^b = K_t A_b \boldsymbol{u}_n \Delta t \tag{10}$$

$$\Delta \boldsymbol{F}_{t,i}^b = K_t A_b \boldsymbol{u}_t \Delta t \tag{11}$$

where $\boldsymbol{F}_{n,i}^b$ and $\boldsymbol{F}_{t,i}^b$ are the ith normal and tangential bond forces by the linear spring. A_b is the cross-sectional area of the bond. $\boldsymbol{u}_n$ and $\boldsymbol{u}_t$ are the normal and tangential relative velocities.

$$\Delta \boldsymbol{M}_{n,i}^b = K_t I_p \boldsymbol{\omega}_n \Delta t \tag{12}$$

$$\Delta \boldsymbol{M}_{t,i}^b = K_n I \boldsymbol{\omega}_t \Delta t \tag{13}$$

where $\boldsymbol{M}_{n,i}^b$ and $\boldsymbol{M}_{t,i}^b$ are the ith normal and tangential bond moments by the linear spring. $\boldsymbol{\omega}_n$ and $\boldsymbol{\omega}_t$ are the normal and tangential relative angular velocities.

$$\boldsymbol{F}_n^b = 2\beta\sqrt{M_e K_n}\boldsymbol{v}_n + \sum_i \Delta \boldsymbol{F}_{n,i}^b \tag{14}$$

$$\boldsymbol{F}_t^b = 2\beta\sqrt{M_e K_t}\boldsymbol{v}_t + \sum_i \Delta \boldsymbol{F}_{t,i}^b \tag{15}$$

where $\boldsymbol{F}_n^b$ and $\boldsymbol{F}_t^b$ are the normal and tangential bond forces. β is the damping coefficient. M_e is the particle mass.

$$\boldsymbol{M}_n^b = 2\beta\sqrt{J_s K_t I_p}\boldsymbol{\omega}_n + \sum_i \Delta \boldsymbol{M}_{n,i}^b \tag{16}$$

$$\boldsymbol{M}_t^b = 2\beta\sqrt{J_s K_n I}\boldsymbol{\omega}_t + \sum_i \Delta \boldsymbol{M}_{t,i}^b \tag{17}$$

where $\boldsymbol{M}_n^b$ and $\boldsymbol{M}_t^b$ are the normal and tangential bond moments. J_s is the particle moment of inertia.

$$K_n = \frac{Y_b}{L_b} \tag{18}$$

$$K_t = \frac{K_n}{2(1-\nu)} \tag{19}$$

where K_n and K_t are the normal and tangential stiffness constants. Y_b and ν are the bond Young's modulus and Poisson's ratio, respectively.

3.3 Model Descriptions

A simple wedge-shaped fracture is shown in **Figure 2**. Enclosed by rigid and no-slip walls, its length and height are 200 mm by 40 mm while inlet and outlet width are 3 mm and 1 mm, respectively. The particles are inserted at the fracture inlet, which is kept at constant 0.2 MPa. The fracture outlet is kept at 0, which makes the pressure gradient of 1 MPa/m along the fracture. The drilling fluid is assumed to be Newtonian and incompressible with density of 2,000 kg/m^3. The particle density, Young's modulus, Poisson's ratio. friction coefficient, and restitution coefficient are 2,500 kg/m^3, 1 GPa, 0.3, 0.5, 0.5, respectively. The LCM concentration is 10% by volume. Because of the pressure gradient, the fluid only flows from the inlet to the outlet. Gravity takes effect in the downward direction of 9.81 m/s^2 magnitude.

Based on the PISO (Pressure-Implicit with Splitting of Operators) algorithm, the unresolved solver is utilized to solve the governing equations (Issa, 1986). The mesh size in the unresolved algorithm needs to be larger than particle diameters. Otherwise, the convergence of porosity calculation would yield a value smaller than a minimum packing porosity. At the same time, if the mesh size were too large, the fluid pressure and velocity calculations would not be accurate. To ensure the accuracy of the simulation results, the mesh size is set to be 3 mm by 3 mm by 1 mm (length by height by width).

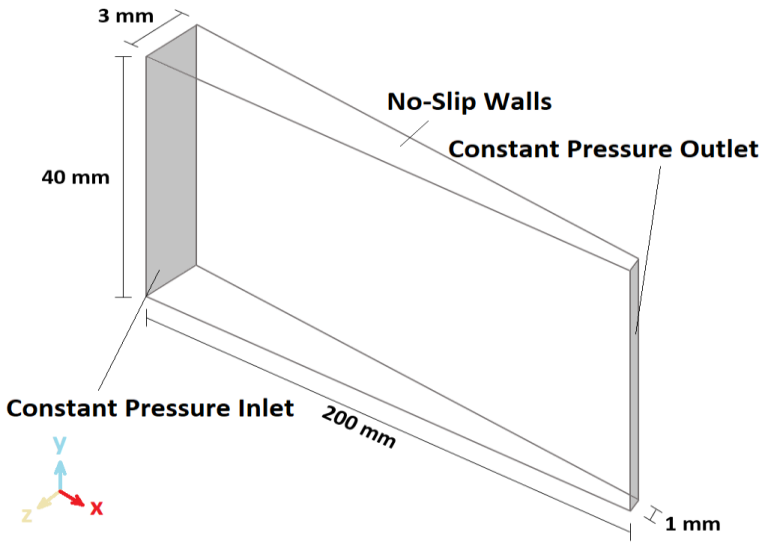

Figure 2: A 3D representation of the fracture geometry enclosed by rigid and no-slip walls. The particles are inserted at the inlet and flow towards the outlet. Both the inlet and outlet pressure are constant. The pressure gradient along the fracture is 1 MPa/m.

4. RESULTS AND DISCUSSION

4.1 Fracture Sealing on Particle Size Distribution

The particles released at the inlet begin flowing to the outlet due to the pressure gradient along the longitudinal direction of the fracture. During the transport process, the LCMs interact with their surroundings including the fracture walls and the neighboring particles. This frequent collisions and shearing are experienced by most of the LCMs. In the cases of uniform particle sizes where there are no sufficient large particles, fracture sealing cannot be achieved. The importance of particle size in fracture sealing has been investigated previously on uniformly sized LCMs (Lee and Dahi Taleghani, 2020). Size distributions on the LCM formula can also influence the fracture sealing capability. As illustrated in **Figure 3**, uniformly sized particles cannot minimize the fluid loss rate at the fracture outlet, whereas the blends of other LCM formula with some percentage of small particles would improve its result. The fluid loss rate, q_{out}, is in cubic meter per second in the y-axis. The x-axis represents the dimensionless volume, which is defined as the ratio of the injection volume to the fracture volume.

In geothermal wells, the conventional LCMs experience size degradation. The effect can be the reduction of equivalent diameter or the change in the sphericity. This is a key factor in fracture sealing. When the size distribution is changed due to thermal effects, the original design that is meant for the targeted region needs to be reconsidered for the quality of the sealing zone. Although the simulation is conducted in an isothermal condition, we have included various particle sizes to account for the size degradation.

By adding a small portion of small particles into the size distribution, it can greatly promote the bridging and sealing process. First, a bridge begins to form at a certain depth inside the fracture as particles clump together and become a pack by the adhesive forces upon contacts. This would result in a pressure drop and further slow down the transport of the trailing LCMs. Second, once the initial bridged location is established, the trailing LCMs would settle and accumulate behind the pack. Then, this pack of particles would grow in size and fill up the fracture space until the insertion is no longer possible. As shown in **Figure 4**, the fracture is filled with LCMs of various sizes, and a group of particle pack can be seen at the outlet. Their contact forces are shown between the tightly packed LCMs. During the transport process, the fluid rate peaks until the initial bridging occurs, causing the overall flow rate to decrease. As shown in **Fig. 5**, the flow rate begins to decrease as the front particles slow down to form a bridge. The flow rate continues to decline as more LCM particles build up at the bridged location. The flow rate only stays constant when the particle insertion is no longer possible, or the particle accumulate all the way to the inlet.

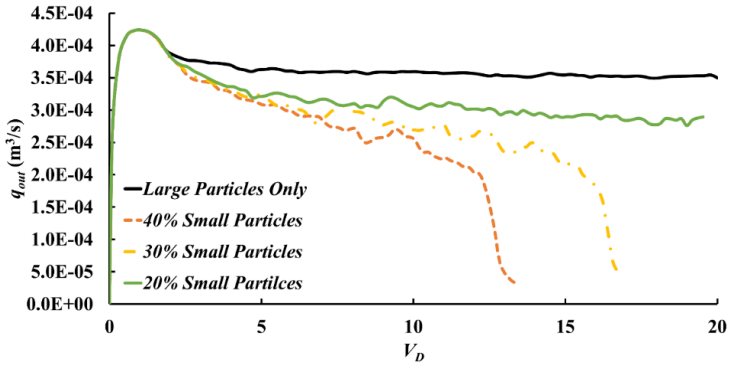

Figure 3: Fluid loss rates of different LCM blends. Fracture sealing is enhanced by adding some size variations in the distribution.

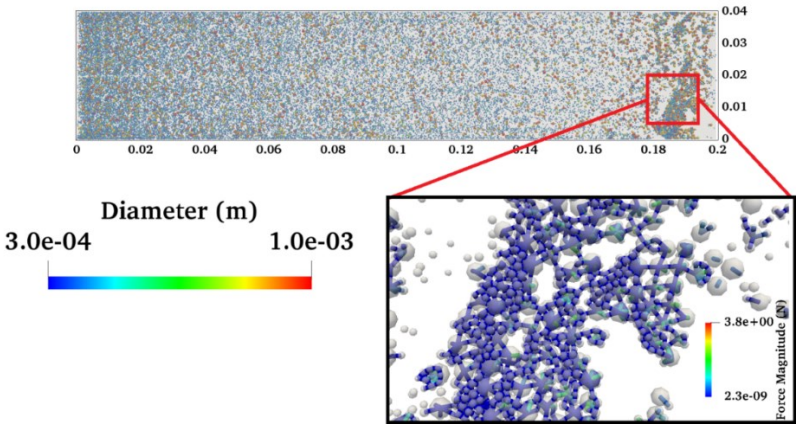

Figure 4: Initial bridge by a pack of particles forming together. Their interaction forces can be seen between the tightly packed LCMs.

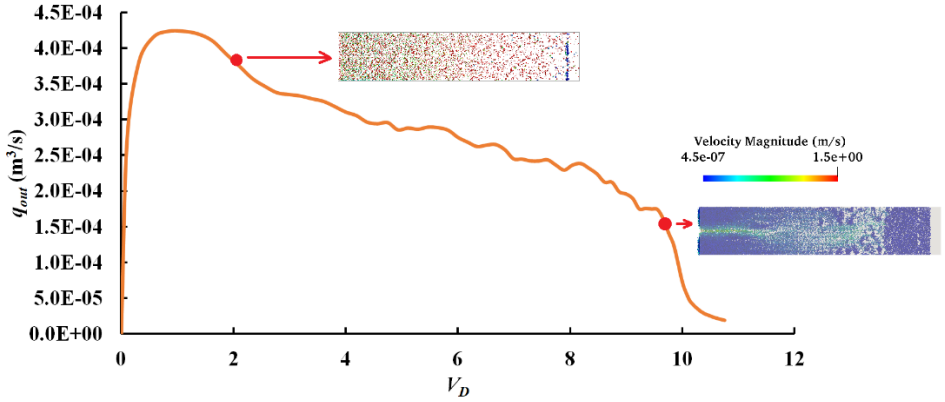

Figure 5: Fluid loss rate of fracture sealing. Flow rate declines as the fracture is bridged and sealed. Particle velocities also decrease during the fracture sealing process.

4.2 Mixture of Granular and Fibrous LCMs

The main objective of the LCM inclusion in drilling formula is to minimize fluid loss, to prevent any damage to the formation, and to maintain the well integrity. Different types of the LCMs may provide different mechanisms in fracture sealing. The simulation studies on fibrous LCMs show successful fracture sealing results. Fiber particles are created by bonding the spherical particles together in a rod-like shape. In this study, fibers of an aspect ratio of four are mixed with granular LCMs. The size of individual spheres in a fiber particle can also vary. On average, slight improvements in fluid losses are obtained. Although the results of every simulation may vary, an

improvement about 10% in total fluid loss from pure granular to a combined granular-fiber LCMs can be seen in **Figure 6**. This decrease in total fluid loss is due to a faster bridging process of the fiber blends, which also confirms the theory of mat-like bridge formed by the fibers. Additionally, there is a large pressure drop across the bridged location, making the flow of trailing particles even slower. A second bridging location is therefore formed near the fracture inlet. A snapshot of a sealed fracture and its velocity map are shown in **Figure 7**. It is interesting that at the bridging location near the inlet, the LCMs accumulate on the top and bottom, leaving the middle with the highest velocity.

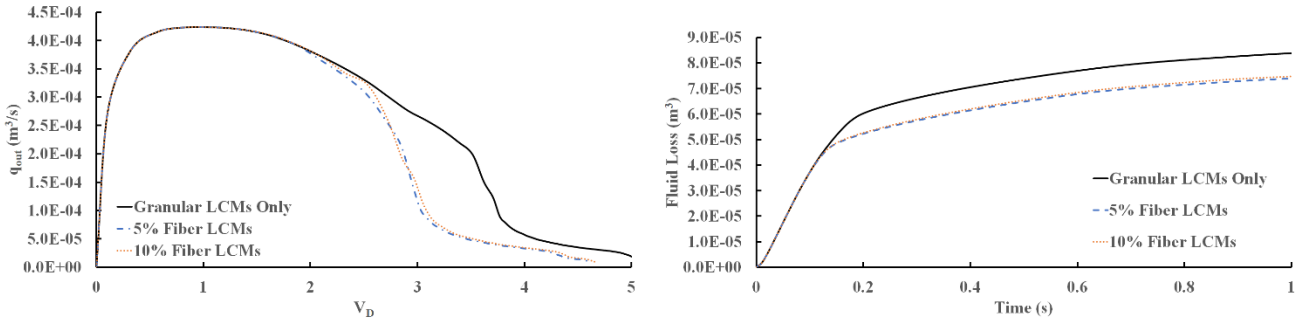

Figure 6: Results of fluid rate and fluid loss from different cases. Frist case only has granular LCMs while the second and the third case has 5% and 10% fibers, respectively.

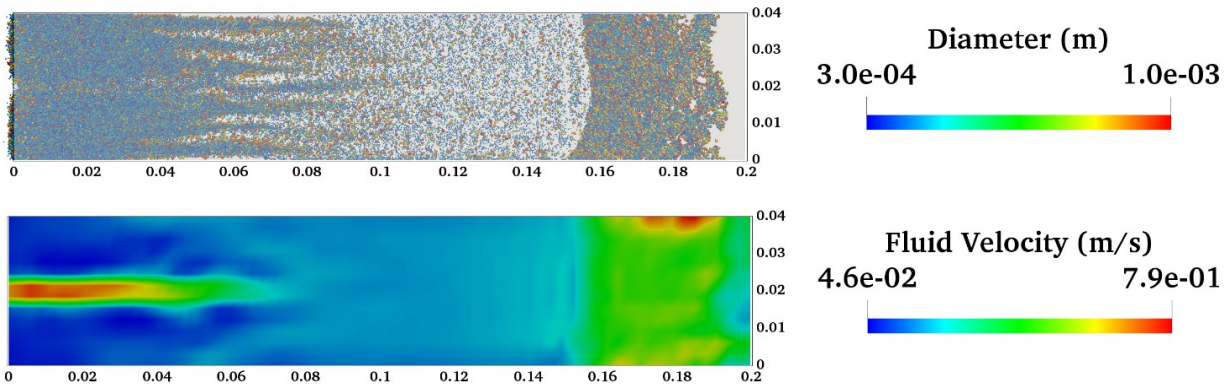

Figure 7: Fracture sealing and its corresponding velocity map. First bridging location is near the fracture outlet while the other bridging location is formed around the inlet.

5. CONCLUSIONS

This numerical simulation study focuses on the fracture sealing capability of various LCM sizes by the coupled CFD-DEM. In the combined Eulerian-Lagrangian approach, individual particle-particle and particle-fluid momentum transfers are possible. This model assumes that the LCMs can reach to the outlet and plug up the fracture instead of the fracture face. As a result, the cases where fluid loss cannot be reduced is due to insufficient particle sizes, and the LCMs would get flushed out without a chance to accumulate and settle inside the fracture. On the other hand, fracture sealing is possible when there is sufficient number of large LCMs to help form the first bridge.

It is the first time that the fibrous LCMs are tested in a coupled CFD-DEM simulation. The model uses the flexible rod-like approach to create fiber particles by bonding multiple spheres. A mixture of fibrous and granular particles exhibits a good sealing capability. Although only the fibers with the aspect ratio of four are simulated, they perform better and show less fluid loss than the performance of the pure granular blend. All in all, the CFD-DEM is a suitable simulation tool for non-granular particulate flow. Longer chains of fibers and materials with irregular shapes can be tested in the future.

ACKNOWLEDGEMENT

This material is based upon work supported by the U.S. Department of Energy's Office of Energy Efficiency and Renewable Energy (EERE) under the Geothermal Program Office, Award Number DE EE0008602. The authors appreciate DOE support.

REFERENCES

Abrams, A.: Mud Design to Minimize Rock Impairment Due to Particle Invasion, *Journal of Petroleum Technology*, **29**, (1977), 586-592.

Alsaba, M., Al Dushaishi, M. F., Nygaard, R. et al.: Updated Criterion to Select Particle Size Distribution of Lost Circulation Materials for An Effective Fracture Sealing. *Journal of Petroleum Science and Engineering*, **149**, (2017), 641-648.

Amanullah, M., Arfaj, M., and Alouhali, R.: Novel Plant-Based Particulate and Fibrous LCM Products for Loss Control While Drilling, International Petroleum Technology Conference, Beijing, China, March 26-28, (2019).

Arena, U., D'Amore, M., and Massimilla, L.: Carbon Attrition during the Fluidized Combustion of Coal, *AlChE Journal*, **29**, (1983), 40-49.

Baret, J.-F., Daccord, G., and Yearwood, J.: Cement/Formation Interactions, Well Cementing, *Developments in Petroleum Science*, **28**, (1990).

Carson, C. C. and Lin, Y. T.: Impact of Common Problems in Geothermal Drilling and Completion, Annual Geothermal Resources Council Meeting, San Diego, California, USA, October 11, (1982).

Chellappah, K. and Aston, M. S.: A New Outlook on the Ideal Packing Theory for Bridging Solids, SPE International Symposium and Exhibition on Formation Damage Control, Lafayette, Louisiana, February 15-17, (2012).

Cole, P., Young, K., Doke, C. et al.: Geothermal Drilling: A Baseline Study of Nonproductive Time Related to Lost Circulation, *Proceedings*, 42nd Workshop on Geothermal Reservoir Engineering, Stanford University, Stanford, CA (2017).

Cundall, P. A. and Strack, O. D. L.: A Discrete Numerical Model for Granular Assemblies, *Géotechnique*, **29**, (1979), 47-65.

Di Felice, R.: The Voidage Function for Fluid-Particle Interaction Systems, *International Journal of Multiphase Flow*, **20**, (1994), 153-159.

Dick, M.A., Heinz, T.J., Svoboda, C.F., and Aston, M.: Optimizing the Selection of Bridging Particles for Reservoir Drilling Fluids, SPE International Symposium on Formation Damage Control, Lafayette, Louisiana, February 23-24, (2000).

Finger, J. and Blankenship, D.: *Handbook of Best Practices for Geothermal Drilling*, (2010).

Furnas, C. C.: Grading Aggregates - I. - Mathematical Relations for Beds of Broken Solids of Maximum Density, *Industrial and Engineering Chemistry*, **23**, (1931), 1052-1058.

Goniva, C., Kloss, C., Deen, N. G. et al.: Influence of Rolling Friction on Single Spout Fluidized Bed Simulation, *Particuology* **10**, (2012), 582-591.

Goodman, M. A.: *Lost Circulation in Geothermal Wells: Survey and Evaluation of Industry Experience*, (1981).

Grant, P., Lassus, L., Savari, S., and Whitfill, D. L.: Size Degradation Studies of Lost Circulation Materials in A Flow Loop, IADC/SPE Drilling Conference and Exhibition, Fort Worth, TX, March 1-3, (2016).

Guo, Y., Curtis, J., Wassgren, C., et al.: Granular Shear Flows of Flexible Rod-Like Particles, *AIP Conference Proceedings*, **1542**, (2013), 491-494.

Guo, Y., Wassgren, C., Hancock, B., et al.: Validation and Time Step Determination of Discrete Element Modeling of Flexible Fibers, *Powder Technology*, **249**, (2013), 386-395.

Hands, N., Kowbel, K., Maikranz, S., and Nouris, R.: Drill-in Fluid Reduces Formation Damage, Increases Production Rates. *Oil & Gas Journal*, **96**, (1998), 65–69.

Issa, R. I.: Solution of the Implicitly Discretised Fluid Flow Equations by Operator-Splitting, *Journal of Computational Physics*, **62**, (1986), 40-65.

Kaeuffer, M.: Determination de L'Optimum de Remplissage Granulometrique et Quelques Proprietes S'y Rattachant, Congres International de I'A.F.T.P.V., Rouen, France. October, (1973).

Kang, Y., Tan, Q., You, L. et al.: Experimental Investigation on Size Degradation of Bridging Material in Drilling Fluids, *Powder Technology*, **342**, (2019), 54-66.

Kloss, C., Goniva, C., Hager, A. et al.: Models, Algorithms, and Validation for Opensource DEM and CFD-DEM, *Progress in Computational Fluid Dynamics* **12**, (2012), 140-152.

Kumar, A., Chellappah, K., Aston, M., and Bulgachev, R.: Quality Control of Particle Size Distributions, SPE European Formation Damage Conference and Exhibition, Noordwijk, the Netherlands, June 5-7, (2013).

Lavrov, A.: *Lost Circulation: Mechanisms and Solutions*, (2016).

Lecolier, E., Herzhaft, B., Rousseau, L. et al.: Development of A Nanocomposite Gel for Lost Circulation Treatment, SPE European Formation Damage Conference, Sheveningen, the Netherlands, May 25-27, (2005).

Lee, L. and Dahi Taleghani, A.: Simulating Fracture Sealing by Granular LCM Particles in Geothermal Drilling, *Energies*, **13**, (2020), 4878.

Lin, C.-L. and Wey, M.-Y.: Influence of Hydrodynamic parameters on Particle Attrition during Fluidization at High Temperature, *Korean Journal of Chemical Engineering*, **22**, (2005), 154-160.

Loeppke, G. E., Glowka, D. A., and Wright, E. K.: Design and Evaluation of Lost-Circulation Materials for Severe Environments, *Journal of Petroleum Technology*, **42**, (1990), 328-337.

Mansour, A. K., Ezeakacha, C., Dahi Taleghani, A. et al.: Smart Lost Circulation Materials for Productive Zones, SPE Annual Technical Conference and Exhibition, San Antonio, Texas, October 9-11, (2017).

Mansour, A. K. and Dahi Taleghani, A.: Smart Loss Circulation Materials for Drilling Highly Fractured Zones, SPE/IADC Middle East Drilling Technology Conference and Exhibition, Abu Dhabi, UAE, January 29-31, (2018).

Messenger, J. U.: *Lost Circulation*, (1981).

Potyondy, D. O., and Cundall, P. A.: A Bonded-Particle Model for Rock, *International Journal of Rock Mechanics & Mining Sciences*, **41**, (2004), 1329-1364.

Razavi, O., Vajargah, A. K., van Oort, E. et al.: Optimum Particle Size Distribution Design for Lost Circulation Control and Wellbore Strengthening, *Journal of Natural Gas Science and Engineering*, **35A**, (2016), 836–850.

Redden, J.: Advanced Fluid Systems Aim to Stabilize Well Bores, Minimize Nonproductive Time, *The American Oil & Gas Reporter*, **52**, (2009), 58-65.

Schramm, M., Tekeste, M. Z., Plouffe, C., and Harby, D.: Estimating Bond Damping and Bond Young's Modulus for A Flexible Wheat Straw Discrete Element Method Model, *Biosystems Engineering*, **186**, (2019), 349-355.

Scott, P. D., Beardmore, D. H., Wade, Z. D. et al.: Size Degradation of Granular Lost Circulation Materials, IADC/SPE Drilling Conference and Exhibition, San Diego, CA, March 6-8, (2012).

Smith, P.S., Browne, S.V., Heinz, T.J., and Wise, W.V.: Drilling Fluid Design to Prevent Formation Damage in High Permeability Quartz Arenite Sandstones, SPE Annual Technical Conference and Exhibition, Denver, Colorado, October 6–9, (1996).

Vickers, S., Cowie, M., Jones, T., and Twynam, A. J.: A New Methodology That Surpasses Current Bridging Theories to Efficiently Seal A Varied Pore Throat Distribution as Found in Natural Reservoir Formations, AADE Drilling Fluids Technical Conference, Houston, Texas, April 11-12, (2006).

Whitfill, D.: Lost Circulation Material Selection, Particle Size Distribution and Fracture Modeling with Fracture Simulation Software, IADC/SPE Asia Pacific Drilling Technology Conference and Exhibition, Jakarta, Indonesia, August 25-27, (2008).

Yang, M., and Chen, Y.: Investigation of LCM Soaking Process on Fracture Plugging for Fluid Loss Remediation and Formation Damage Control, *Journal of Natural Gas Science and Engineering*, **81**, (2020).

Zhu, H. P., Zhou, Z. Y., Yang, R. Y., and Yu, A. B.: Discrete Particle Simulation of Particulate Systems: Theoretical Developments, *Chemical Engineering Science*, **62**, (2007), 3378-3396.

Zhu, H. P., Zhou, Z. Y., Yang, R. Y., and Yu, A. B.: Discrete Particle Simulation of Particulate Systems: A Review of Major Applications and Findings, *Chemical Engineering Science*, **63**, (2008), 5728-5770.